Influence of small-scale structure on radiative transfer and photosynthesis in vegetation canopies

Yuri Knyazikhin,[1] Jörn Kranigk,[2] Ranga B. Myneni,[1] Oleg Panfyorov,[2] and Gode Gravenhorst[2]

Abstract. The use of Beer's law to describe the radiation regime in plant canopies is valid for a sufficiently large volume filled densely with phytoelements. This set a limit to the scale at which models, based on Beer's law, can account for structural features of vegetation canopies and provide an adequate prediction of the radiation regime. The aim of our paper is to analyze radiation interaction in vegetation canopies and consequent photosynthetic rates at a scale at which Beer's law loses its validity. We use fractals to simulate the structure of vegetation canopies at this scale. It is shown that both the radiation regime and the photosynthesis depend on the fractal dimension of the plant stand. The development of radiative transfer models in fractal-like media as well as measurements and modeling of fractal characteristics of trees and tree communities are essential for better understanding and scaling of radiative transfer and photosynthetic processes from an individual leaf to the canopy.

1. Introduction

The structure of vegetation canopies determines the spatial distribution of intercepted incident radiation which drives various physiological and physical processes required for the functioning of plants. In order to quantitatively model this functioning, it is important to understand the interaction of electromagnetic radiation with different types of canopy structural organizations.

Numerous models for describing the radiation regime of vegetation canopies have been developed since the classical model of *Monsi and Saeki* [1953], which essentially is Beer-Bouguer's law applied to plant canopy (hereinafter referred to as Beer's law). A key assumption underlining this law is the following: the number of scattering centers (e.g., leaves) in an elementary volume is proportional to its volume. Given leaf size, orientation, and optical properties of leaves, we can mathematically express the law of energy conservation. From information on the spatial distribution of such elementary volumes, one can derive various models for describing the radiation regime of plant stands. For example, in the turbid medium models, the vegetation canopy is treated as a gas with nondimensional planar scattering centers [*Ross*, 1981]. Alternately, modeling plants or trees in a stand as geometrical objects (cones, ellipsoids, etc.) leads to a family of geometrical-optical models [*Nilson*, 1977; *Li and Strahler*, 1986]. There are also hybrid canopy radiation models which incorporate features of both these approaches [*Norman and*

Welles, 1983; *Nilson* 1992; *Li et al.*, 1995; *Myneni et al.*, 1990] and account for some structural properties of tree organization [*Oker-Blom*, 1991; *Chen et al.*, 1994; *Stenberg*, 1995].

Recent investigations of plant morphology [*de Reffye et al.*, 1991] as well as small-scale measurements of geometrical features of individual trees and tree communities [*Zeide and Pfeifer*, 1991; *Rigon et al.*, 1994; *Vedyushkin*, 1995] indicate that the architecture of most vegetation canopies obeys the laws of fractal geometry. The fractal characteristics of vegetation canopies depend on the structure of tree organization and may vary between trees and tree species [*Zeide and Pfeifer*, 1991]. Fractality essentially means that the relationship between volume and number of phytoelements in it is nonlinear. This property conflicts with the above mentioned assumption of Beer's law, and an investigation of its consequence is essential for better understanding of the processes governing the functioning of vegetation systems. Therefore our goal is to analyze the interaction of electromagnetic radiation with fractal-like canopy organizations and to demonstrate that the radiation regime and canopy photosynthesis depend on fractal characteristics of such media, while the Beer's law is insensitive to them.

Here we proceed with the suggestion that a vegetation canopy obeys the laws of fractal geometry and for which there is adequate empirical basis [*Kranigk and Gravenhorst*, 1993; *Kranigk et al.*, 1994]. Thus we use this geometry to reproduce an example coniferous stand with a high level of realism (section 2). We then formulate a strict mathematical definition of vegetation canopy structure as well as a method for its approximation. We utilize the steady state radiative transfer equation to simulate the three-dimensional distribution of photosynthetically active radiation (PAR) and canopy photosynthesis, using the simulated fractal forest as input. The use of transport theory presupposes that Beer's law can be applied

[1]Department of Geography, Boston University, Massachusetts.
[2]Institute of Bioclimatology, University Göttingen, Göttingen, Germany.

to describe the radiative regime in plant canopies; but this assumption is violated in the case of the modeled fractal forest stand. This discrepancy leads to a paradox [*Kranigk*, 1996]: the more accurately the canopy structure is reproduced, the more inaccurately the radiative regime and canopy photosynthesis are estimated (section 3). Note that similar paradoxes are already described and explained, for example, in cloud physics, remote sensing, and microphysiological investigations [*Quattrochi and Goodchild*, 1997; *Lovejoy and Schetzer*, 1994; *Ehleringer et al.*, 1993]. We will follow the methodology of these investigations. We start our analysis with examining the problem of photon interaction with the simplest fractal organization, the Cantor set (section 4). Further, two patterns of canopy organization are considered in section 5. In the first case, the phytoelements are distributed uniformly within the canopy space, and in the second case, their vertical distribution is specified by the distribution of the Cantor set. For both of these patterns, we derive equations for canopy transmittance and photosynthesis which depend on the fractal dimension of the patterns. Finally, a discussion with conclusions about radiation interaction with fractal-like media are presented in section 6.

2. Structure of the Forest Stand in Lange Bramke

Norway spruce stand, about 50 km east of Göttingen in the Harz Mountains, was chosen for simulation (Lange Bramke, 51.85°N, 10.40°E). The watershed, Lange Bramke, where ecosystem measurements were carried out, consists mainly of two slopes with north and south orientation. The base plot, selected for this study, was a 40 m by 40 m plot containing 297 trees (tree density of 1856 trees per hectare) and located on the south slope. The diameters of the tree trunks varied from 6 to 28 cm. The stand is rather dense but with some local gaps. Tree locations were mapped [*Kranigk et al.*, 1994], and total height, height-to-crown base, and crown widths were measured on all trees in this stand.

The trees were divided into five classes with respect to the stem diameter. A model of a Norway spruce based on fractal geometry [*Kranigk and Gravenhorst*, 1993] was then used to build a representative tree in each class. The computer-generated base plot is shown in Figure 1. In the framework of an earlier project, 10 Norway spruce trees near the base plot were cut in 1989 and a data bank on measured crown morphology was assembled [*Gruber et al.*, 1992]. These data were used to validate the architectural and morphological properties of our tree models. A good agreement between measured and simulated tree morphology was reported previously [*Kranigk et al.*, 1994]. Thus we idealize our base plot as a forest canopy consisting of 297 fractal trees (Figure 1). This model of plant stand is used to generate a three-dimensional distribution of photosynthetically active radiation and canopy photosynthesis. A good agreement between the field measurements and the simulated radiation regime at a scale at which Beer's law can be utilized were reported previously [*Kranigk*, 1996; *Knyazikhin et al.*, 1997].

2.1. Basic Foliage Element

A conifer needle is taken as the basic foliage element and approximated as small cylinders. The projected needle area is used to quantify the one-side area of the phytoelements and to
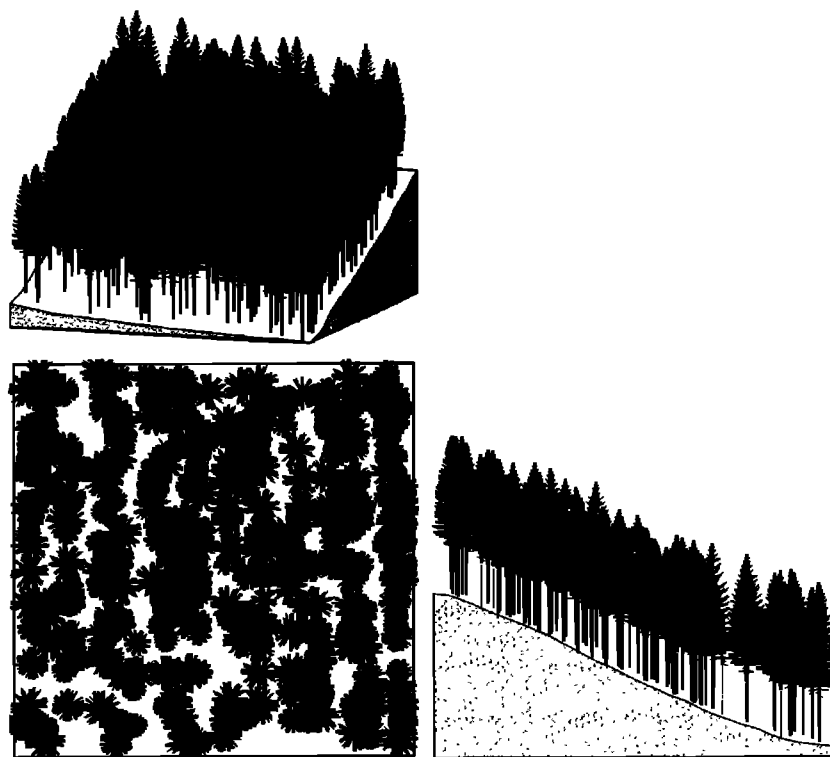

Figure 1. Computer-generated Norway spruce stand shown from different directions: front view (top left), crown map (bottom left), and cross section (right).

express photosynthetic rates. The leaf normal distribution is assumed spherical. The Bi-Lambertian reflectance model [*Ross and Nilson*, 1968] is used in the calculations to simulate the reflection and transmission of needles at PAR wavelengths; the reflectance and transmittance coefficients were determined from measurements (0.067 and 0.033, respectively). Interaction of radiation with stems and branches is neglected; therefore the canopy space is idealized as optically nearly black, flat linear elements that are spherically oriented. Their spatial distribution is generated by the fractal architectural model (Figure 1).

2.2. Canopy Structure and Its Approximation

To quantify the structure of canopy, we introduce an indicator function $\chi(r)$ whose value is 1, if there is a needle at the point $r = (x, y, z)$, and 0 otherwise. The canopy structure is defined by the indicator function. We introduce a fine spatial mesh by dividing the base plot into N_ε nonoverlapping fine cells, e_i, $i = 1, 2, ..., N_\varepsilon$, of size $\Delta x = \Delta y = \Delta z = \varepsilon$. We approximate the canopy structure by a piece-wise constant function $\chi_\varepsilon(r)$: $\chi_\varepsilon(r) = \chi_{\varepsilon,i}$ if $r \in e_i$. Here $\chi_{\varepsilon,i}$ is equal to 1, if there is a needle within the cell e_i, and 0 otherwise. It is intuitively clear that as ε becomes smaller, the function $\chi_\varepsilon(r)$ approximates the canopy structure better. We call this function $\chi_\varepsilon(r)$ an approximation of canopy structure by cells of size ε. Figure 2 demonstrates the three-dimensional distribution of the function $\chi_\varepsilon(r)$, where the cell size ε is 0.5 m. The model of plant stand shown in Figure 1 is the limit of this function as ε tends to zero.

In models of radiation interaction in vegetation canopies, the leaf area density distribution function $u_L(r)$ quantifies the canopy structure. Its value at a fine cell e_i is defined as the
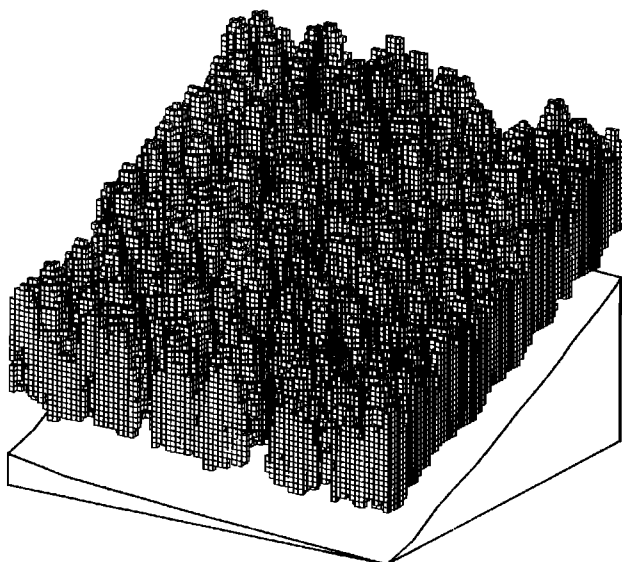

Figure 2. Three-dimensional distribution of foliated cells. The canopy space is limited by the slope and a plane parallel to the slope at a height of the tallest tree. This distribution is described by the function $\chi_\varepsilon(r)$ whose value is 1 (a fine cell is plotted), if there is a needle in the cell around the space point $r=(x,y,z)$, and 0 otherwise (a fine cell is not plotted). The size ε of the fine cell is 0.5 m in this plot. Tending the cell size to zero, this plot converges to the one shown in Figure 1.

ratio of total one-side leaf area within this cell, ΔS_i (in m^2), to the volume ε^3 of this cell [*Ross*, 1981]; that is,

$$u_L(r) = \Delta S_i/\varepsilon^3 \quad \text{if } r \in e_i. \qquad (1)$$

The total one-side leaf area ΔS_i in an infinitesimal cell is comparable to $\Delta x \Delta y = \varepsilon^2$. Therefore the leaf area distribution function becomes arbitrarily large as ε tends to zero. This property sets a limit to the applicability of the classical approach for characterizing the vegetation canopy structure: the cell size should be so great that leaves in it can be treated as infinitesimal planar elements. The heterogeneity of the entire canopy is characterized by variations in leaf area in these cells.

The second conceptual limitation in classical theory is that the leaves are assumed distributed such that there is no mutual shading along any direction. It means that each cell is idealized as a turbid medium filled with infinitesimal planar elements, uniformly distributed within the cell, and oriented in all possible directions. The leaf area density in the cell depends on foliage clumping, gap distribution, etc. This assumption can be realized only if the definition of the leaf area density distribution function can be formulated for arbitrary small cells.

Under these assumptions, Beer's law can be utilized to describe radiation attenuation. The theory allows us to extend its utilization from a sufficiently big cell to the entire canopy [*Ross*, 1981]. The underlying assumptions of Beer's law predetermine a scale at which this approach provides an adequate prediction. There are scales which account for spatial distribution of trees, tree shape, vertical distribution of foliage within crowns, and its clumping [*Knyazikhin et al.*, 1997]. For photosynthesis calculations, however, these scales may be rather large. Canopy photosynthesis depends on the distribution of radiation on foliage elements and the photosynthetic response of the elements. Recent models are capable of reproducing the canopy architecture with a high level of realism, from leaf to canopy scale (for example, Figure 1). The classical transport theory, however, is not useful for predicting the radiation regime at the leaf level. To demonstrate this, we evaluate canopy photosynthesis for two values of the cell size using the classical approach.

3. Canopy Photosynthesis Evaluated With Beer's Law

Let us consider two approximations, $\chi_{0.5}(r)$ and $\chi_{0.25}(r)$, of simulated base plot with cells of size $\varepsilon = 0.5$ m and $\varepsilon=0.25$ m. We use (1) to derive the three-dimensional distribution of leaf area density $u_L(r)$ for these two canopies. The leaf area density of a cell from the intersection of trees is given by the sum of leaf area densities of the intersecting cells. Thus the approximations have the same leaf area as the base plot. Figure 2 illustrates the three-dimensional distribution of the function $\chi_{0.5}(r)$. The histograms of the frequency $v(u)$ of leaf area per foliated cell u for the two approximations are shown in Figure 3. Cells where $u=0$ make up about 77% ($\varepsilon=0.5$ m) and 78% ($\varepsilon = 0.25$ m) of the total number of cells. The
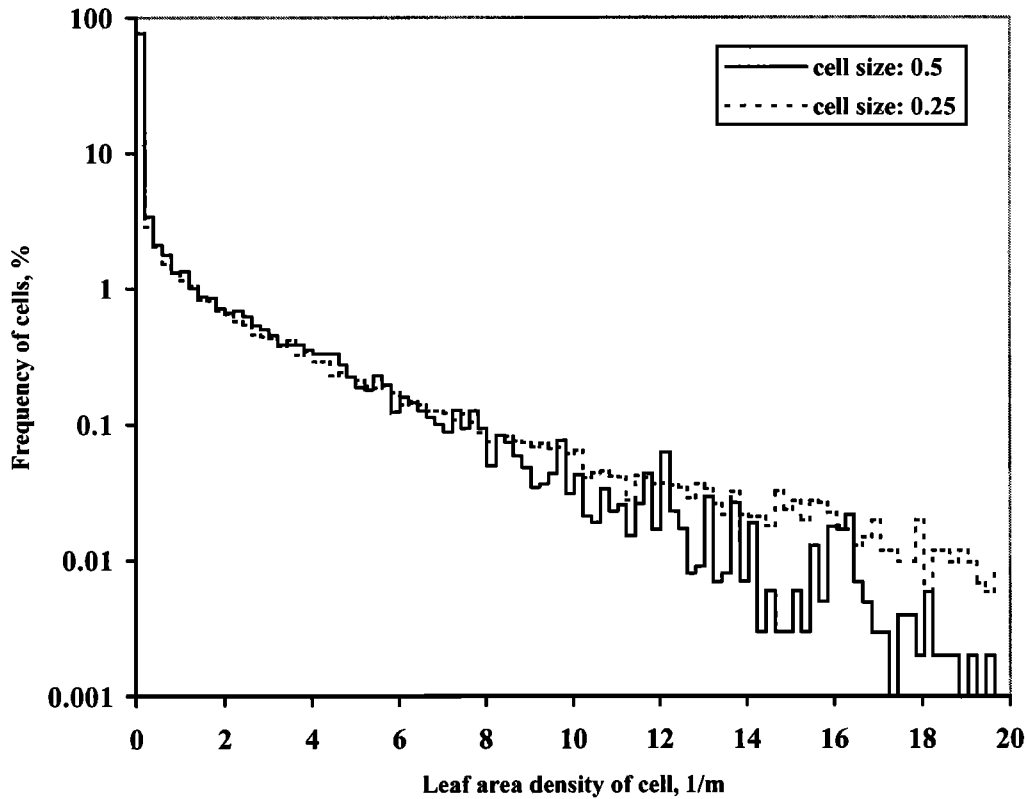
Figure 3. Frequency of leaf area density values.

volume of the parallelepiped in which the tree crowns are located makes up about 27% of the canopy space, which is close to the volume of all foliated cells. Thus the base plot is rather dense but with some local gaps. The average one-side leaf area per unit volume increases from about 0.5 m^2/m^3 to about 0.6 m^2/m^3 when the cell size is halved. Cells of size 0.25 m result in 1.6 times more cells with high foliage densities ($u > 8$ m^2/m^3) than cells of size 0.5 m (Figure 3). These cells are about 1.1% ($\varepsilon = 0.5$ m) and 1.8% ($\varepsilon = 0.25$ m) of the total canopy space. The distribution of cells with low foliage densities ($u < 8$ m^2/m^3) is approximately the same.

We used the steady state radiative transfer equation [*Knyazikhin et al.*, 1997] to simulate the radiation field in the base plot. Its solution is the intensity $I(r,\Omega)$ of PAR. The PAR intensity was evaluated in 80 directions distributed over the unit sphere according to Carlson's quadrature rule [*Carlson*, 1970]. Within the cell about r, a photosynthesis-radiation response $P_{leaf}(r,\Omega_L)$ of leaf area with unit normal Ω_L directed outward from its upper surface was simulated by a three-parameter equation [*Prioul and Chartier*, 1977]:

$$\theta P_{leaf}^2(r,\Omega_L) - (\alpha F_L + P_{max})P_{leaf}(r,\Omega_L) + \alpha F_L P_{max} = 0,$$

where $P_{leaf}(r,\Omega_L)$, α, P_{max} are gross photosynthesis, apparent quantum yield, and maximum gross photosynthesis at light saturation, respectively; θ is the convexity parameter, and F_L is the PAR energy flux on the leaf area with unit normal Ω_L within the cell about r:

$$F_L = \int_{4\pi} I(r,\Omega)|\Omega \cdot \Omega_L| d\Omega.$$

Canopy photosynthesis P_{can} at a given time can be expressed as

$$P_{can} = \int_V P_{cell}(r) u_L(r) dr = \sum_{j=1}^{N_c} P_{cell}(r_j) u_j \varepsilon^3, \qquad (2)$$

where V is the canopy space and $P_{cell}(r)$ is the photosynthetic response of unit leaf area within the cell,

$$P_{cell}(r) = \int_{2\pi^+} P_{leaf}(r,\Omega_L) \frac{1}{2\pi} g(\Omega_L) d\Omega_L.$$

Here $g(\Omega_L)$ is the probability density of leaf normal distribution over the upper hemisphere $2\pi^+$, which is assumed spherical distribution, i.e., $g(\Omega_L)=1$.

Thus we define canopy photosynthesis at a given time as the sum of photosynthetic responses of individual cells. It seems clear that as cell size ε is taken smaller and smaller, (2) should account for the photosynthetic response of individual leaves more and more accurately. This, however, is not true.

Figure 4 demonstrates daily variation in canopy photosynthesis on a cloudy (September 16, 1992) and a clear sunny (September 27, 1992) day for two example canopies. The average difference between the daily canopy photosynthesis from the two canopy approximations of the same base plot is about 14% on a cloudy day versus 9% on a sunny day. In both cases the diurnal canopy photosynthesis decreased with decreasing cell size.

Let us analyze the behavior of canopy photosynthesis as the cell size ε tends to zero. The photosynthetic response
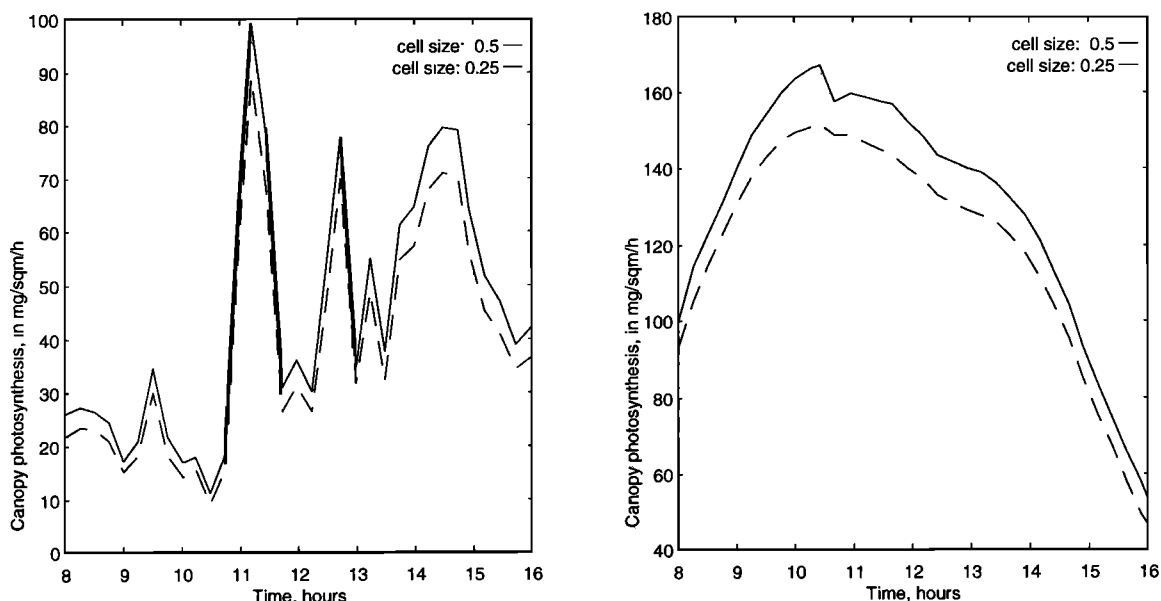
Figure 4. Diurnal variation of canopy photosynthesis on a cloudy (left) and a sunny (right) day for two canopy approximation by cells of the sizes ε=0.5 m and ε=0.5 m.

$P_{cell}(r)$ of unit leaf area may range between zero and its light-saturation rate; that is, $0 \leq P_{cell}(r) \leq P_{max}$. We divide this interval into m subintervals by points P_k: $0 = P_0 < P_1 < ... < P_{m-1} < P_m = P_{max}$. Let $n_\varepsilon(P_j)$ be the number of foliated cells of size ε in which $P_{j-1} \leq P_{cell}(r) < P_j$. We denote by $N_{f,\varepsilon}$ the total number of foliated cells of size ε, i.e., the sum of all $n_\varepsilon(P_j)$. The total one-side leaf area $u(r)dr$ in a sufficiently small cell is comparable to ε^2; that is, $u(r)dr = const \ \varepsilon^2$. We can now rewrite (2) as

$$P_{can} = \sum_{j=1}^{m} P_{j-1} n_\varepsilon (P_{j-1}) const \varepsilon^2 .$$

Taking into account the inequalities $P_j \leq P_{max}, j = 1, 2, ..., m$, it is possible to obtain

$$P_{can} \leq const \varepsilon^2 P_{max} \sum_{j=1}^{m} n_\varepsilon (P_{j-1}) = const P_{max} \varepsilon^2 N_{f,\varepsilon} \quad (3)$$

which does not depend on m.

Figure 5 demonstrates the distribution of points ($\ln(1/\varepsilon)$, $\ln(N_{f,\varepsilon})$) for the largest tree in the simulated base plot; that is, $N_{f,\varepsilon}$ is the total number of foliated cells containing needles of the tree of maximum diameter. These points are well approximated by the linear function $\ln(N_{f,\varepsilon}) = 1.737 \ln(1/\varepsilon) + \ln(227.9)$ with respect to $\ln(1/\varepsilon)$. It follows from this equation that $N_{f,\varepsilon} = 227.9/\varepsilon^{1.737}$. Similar relationships are valid for all trees in our base plot, which can be expressed in the following form:

$$N_{f,\varepsilon,i} = C_i \varepsilon^{-D_i} , \quad i = 1, 2, ..., 5. \quad (4)$$

Here $N_{f,\varepsilon,i}$ is the number of foliated cells of size ε containing needles of the ith representative of the tree class; C_i is a constant that depends on the representative tree, and D_i is the

fractal dimension of the foliage set defined as [*Barnsley*, 1993]

$$D_i = \lim_{\varepsilon \to 0} \frac{\ln N_{f,\varepsilon,i}}{\ln 1/\varepsilon} . \quad (5)$$

The fractal dimension quantifies the internal structure of tree organization and may vary between trees and tree species [*Zeide and Pfeifer*, 1991]. Because needles are approximated as thin cylinders, which are close to a small straight line, the fractal dimension of our simulated trees is less then 2; that is, $D_i < 2$. Substituting (4) in (3) and noting that $N_{f,\varepsilon}$ is the sum of $N_{f,\varepsilon,i}$, we can show that

$$P_{can} \leq const P_{max} \ \varepsilon^2 \sum_{i=1}^{5} C_i \varepsilon^{-D_i} \leq const P_{max} \ C \varepsilon^{2-D} .$$

Here $C = max\{C_1, C_2, ... ,C_5\}$, $D = max\{D_1,D_2,...,D_5\}$. Since $2-D > 0$, it follows that P_{can} becomes arbitrarily small as ε tends to zero! Note that no suggestions about radiation model and photosynthesis equation are required to derive the last inequality. It means that such a degeneration holds true for any radiation-photosynthesis model using fractal model of canopy structure.

Thus we obtain the following result: the more accurately canopy structure is reproduced, the more inaccurately canopy photosynthesis is evaluated. We come to the same result when we evaluate the total PAR energy incident on leaves in the canopy. Two reasons may be given for such discrepancies. On the one hand, the number of foliage elements in an elementary volume was assumed proportional to this volume. This allows us to quantify the canopy structure in terms of leaf area density distribution function $u(r)$ which underlies the use of Beer's law in radiation-photosynthesis calculations. On the other hand, we used this method in a canopy in which the
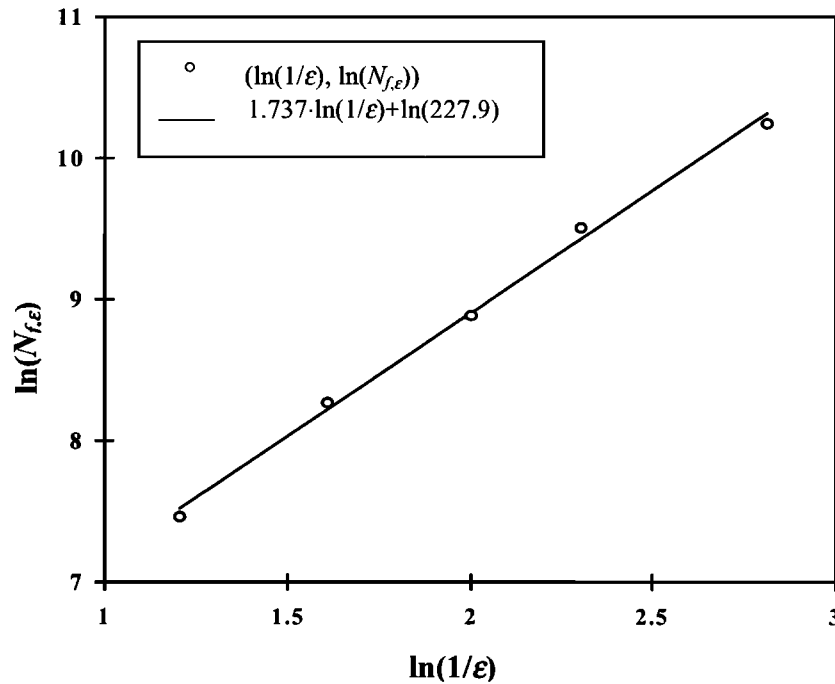
Figure 5. Dependence of $\ln(N_{f,\varepsilon})$ on $\ln(1/\varepsilon)$. The points $(\ln(1/\varepsilon), \ln(N_{f,\varepsilon}))$ are distributed along the linear function with respect to $\ln(1/\varepsilon)$: $1.737 \ln(1/\varepsilon) + \ln(227.9)$.

relationship between the elementary volume and the number of foliage elements in it was nonlinear (equation (4)). If the canopy structure is similar to a fractal-like medium, Beer's law cannot be applied to describe light interaction in forest canopies. An essential revision of existing modeling techniques is needed to correctly simulate such processes in forest canopies. We will attempt to do this next, when we consider radiation interaction in a medium described by the simplest fractal set, the Cantor set.

4. The Cantor Set

We consider the Cantor set that can be obtained by the following iterative procedure. A unit interval [0,1] is divided into three equal subintervals, and the middle subinterval is removed. This transformation is then applied to each of the remaining two intervals (Figure 6). By repeating this transformation n times, we obtain the nth approximation of the Cantor set. Figure 6 demonstrates four successive iterations, each consisting of $M_{\varepsilon,C} = 2^n$ intervals of size $\varepsilon = 1/3^n$ ($n = 0, 1, 2, 3, 4$). As the number of iterations tend to infinity, these intervals degenerate into points. A set of these points is said to be the Cantor set or Cantor's points iterated from the interval [0,1]. In section 5, the Cantor points will be interpreted as foliage elements encountered along the photon path; in this section we discuss some properties of the Cantor set necessary for the discussion in section 5.

We begin with the derivation of a relative distribution function of Cantor's points. Let $F(s)$ be the portion of these points in the interval $[0, s)$. Clearly, $F(0) = 0$ and $F(1)=1$. Because the intervals [0,1/3) and [2/3,1) are transformed by the same algorithm, each of them therefore contains an equal number of Cantor's points (Figure 6). In the interval [1/3,2/3),

there are no Cantor points. Therefore we assign the value 1/2 to the function $F(s)$ when $1/3 \le s < 2/3$. The intervals [0,1/9), [2/9,1/3), [2/3,7/9), and [8/9,1) are also subjected to the transformation by this algorithm, and so each of them contains an equal number of points from the Cantor set. Since the intervals [1/9,2/9) and [7/9,8/9) have no Cantor points, the function $F(s)$ is constant on these intervals, taking on the values 1/4 and 3/4, respectively. By repeating this procedure n times, we obtain the nth approximation of the desired distribution function. The eighth iteration of $F(x)$ is shown in Figure 7. As the number of iterations tend to infinity, we can assign a value to the function $F(s)$ at any point in the interval [0,1].

The relative distribution function of Cantor's points has two important properties. On the one hand, it is a continuous function. On the other hand, it is a piece-wise constant function that can take new values only at Cantor's points. A function satisfying these two properties is defined to be a singular function [Kolmogorov, 1950].

We use the symbol $\chi^C(s)$ to denote the indicator function of the Cantor set; that is, $\chi^C(s)$ takes on the value 1, if there is a point of the Cantor set at the point s ($0 \le s \le 1$), and 0 otherwise. We divide the interval $0 \le s \le 1$ into M_ε equal subintervals, $e_i = [s_{i-1}, s_i)$, by points $s_i = (i-1)\varepsilon$, $i = 1,2,...,M_\varepsilon$, and approximate the indicator function $\chi^C(s)$ by a piece-wise constant function $\chi^C_\varepsilon(s)$; that is, $\chi^C_\varepsilon(s) = \chi^C_{\varepsilon,i}$ if $s_{i-1} \le s < s_i$, $i=1, 2, ..., M_\varepsilon$. Here $\chi^C_{\varepsilon,i}$ is equal to 1, if there is a point of the Cantor set in the interval $[s_{i-1}, s_i)$ and 0 otherwise. The length, Δs (in relative units), of each interval is $\Delta s = \varepsilon$. The function $\chi_\varepsilon(s)$ converges to the indicator function, as ε tends to zero. Let $M_{\varepsilon,C}$ be the number of intervals containing points of the Cantor set. Note that if $\varepsilon = 1/3^n$, then $M_{\varepsilon,C} = 2^n$ (Figure 6). It follows from (5) that the fractal dimension D of the Cantor set is $D = \ln 2/\ln 3 \approx 0.63$.
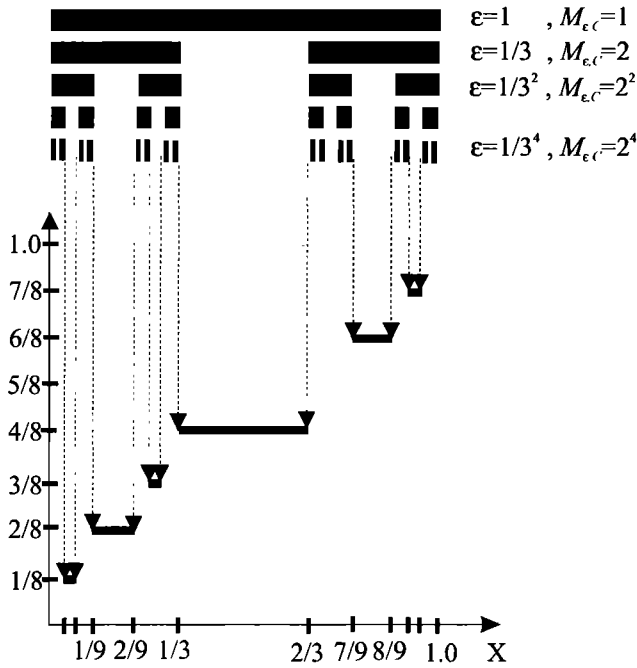
Figure 6. The Cantor set (top) which is obtained by iteratively removing the middle one-third section of the "black" intervals. We describe a distribution of points of the Cantor set in a relative unit taking the total Cantor set as 1 (bottom).

Let us consider the nth approximation of the Cantor set which can be explicitly described by the function $\chi^C_\varepsilon(s)$. We approximate the distribution function of Cantor's points by a piece-wise constant function $F_\varepsilon(s)$: $F_\varepsilon(s) = F_{\varepsilon,i}$ if $s_{i-1} \leq s < s_i$, $i = 1, 2, ..., M_\varepsilon$, where $F_{\varepsilon,i}$ is a portion of Cantor's points in the interval $[0, s_i)$; that is,

$$F_{\varepsilon,i} = F(s_i) = \sum_{k=1}^{i}(F(s_k) - F(s_{k-1})) = \sum_{k=1}^{i} dF(s_k) . \quad (6)$$

It may be shown that this function converges to $F(s)$ as ε tends to zero. The function $F_\varepsilon(s)$ can only be evaluated when the values of $F(s)$ are specified at $M_\varepsilon + 1$ discrete values of its argument. This information, however, may often be unknown in practical situation; for instance, as when one deals with a fractal set like the one used to simulate the tree stand described earlier. The question then arises of whether or not the distribution function of Cantor's points can be approached in terms of $\chi^C_\varepsilon(s)$.

Let us examine the convergence process, $F_\varepsilon(s) \rightarrow F(s)$, when ε takes on values $1/3^n$, $n = 1, 2, ...,$. In this case we have (compare Figure 6)

$$F(s_k) - F(s_{k-1})$$

$$= \begin{cases} \dfrac{1}{2^n}, & \text{if there are points of the Cantor set in } [s_{k-1}, s_k), \\ 0, & \text{otherwise,} \end{cases}$$

$$= \frac{1}{2^n} \chi^C_{\varepsilon,k} . \quad (7)$$

Taking into account the following relationship between the fractal dimension $D = \ln 2/\ln 3 = \ln_3 2$ and the length $\Delta s = \varepsilon = 1/3^n$ (in relative units) of the interval $[s_{k-1}, s_k)$,

$$(\Delta s)^D = \left(\frac{1}{3^n}\right)^{\log_3 2} = \frac{1}{2^n},$$

we can rewrite (7) as

$$dF_\varepsilon(s_k) = \chi^C_\varepsilon(s) (\Delta s)^D, \quad D = \log_3 2 \approx 0.63 . \quad (8)$$

This equation shows that the relation between the length of an elementary interval and the relative number of Cantor's points in this interval is nonlinear. Substituting (8) into (6), we can express $F_\varepsilon(s)$ in terms of the indicator function for the nth approximation of the Cantor set

$$F_{\varepsilon,i} = \sum_{k=1}^{i} \chi^C_{\varepsilon,k}(\Delta s)^D . \quad (9)$$

It will be recalled that this equality, however, is valid only under a special choice of ε, i.e., when $\varepsilon = 1/3^n$. Because the function $F_\varepsilon(s)$ converges to $F(s)$, no matter how ε tends to zero, (9) is approximately satisfied for ε other than $1/3^n$. This formula therefore provides a means of approaching the relative distribution of Cantor's points, using the nth approximation of the Cantor set and its indicator function as input variables. Indeed, it follows from (9) that the portion of Cantor's points in the interval $[0, s_i)$ is the sum of power of the lengths of intervals containing the Cantor points. The value of power coincides with the fractal dimension of the Cantor set.

Equation (9) allows us to introduce a generalized length to measure Cantor's points. Let L be a length of the interval $[0,1]$ expressed in a metric system (e.g., in meters). A length of each subinterval $[s_{i-1}, s_i)$ is $\Delta s L$ in this system. It follows from (9) that

$$F(s L) = F(s) L^D; \quad (10)$$

that is, the portion $F(s)$ (dimensionless) of Cantor's points in the interval $[0,s)$ of the length sL has a generalized length $F(s)L^D$ (e.g., in m^D). Thus the Cantor set iterated from the interval $[0,1]$ of length $L = 1$ m can be assigned the generalized length of 1 m^D, where $D = \log_3 2 \approx 0.63$ is the fractal dimension of the Cantor set. We call this set a unit Cantor set. Therefore if a Cantor set is iterated from an interval of length H, its total generalized length is H^D. The generalized length of its portion $F(s)$ in the interval $[0, s H]$, $0 \leq s < 1$, of length sH is $F(s) H^D$ (e.g., in m^D). From this viewpoint, (9) has a simple interpretation. Indeed, the nth approximation of our Cantor set (e.g., shown in Figure 6) consists of Cantor subsets iterated from subintervals $[s_{i-1}, s_i)$, each of them of length Δs. Equation (9) shows that the generalized length of the whole Cantor set is the sum of the generalized lengths of these Cantor subsets.

The result formulated in terms of (9) can now be utilized to specify a distribution function of fractal-like sets, other than the Cantor set, for example, of the fractal sets shown in Figure 1. This relationship is a special case of the Lebesgue theory of integration known as Lebesgue integral with respect to the Hausdorf measure [*Barnsley*, 1993]. The following
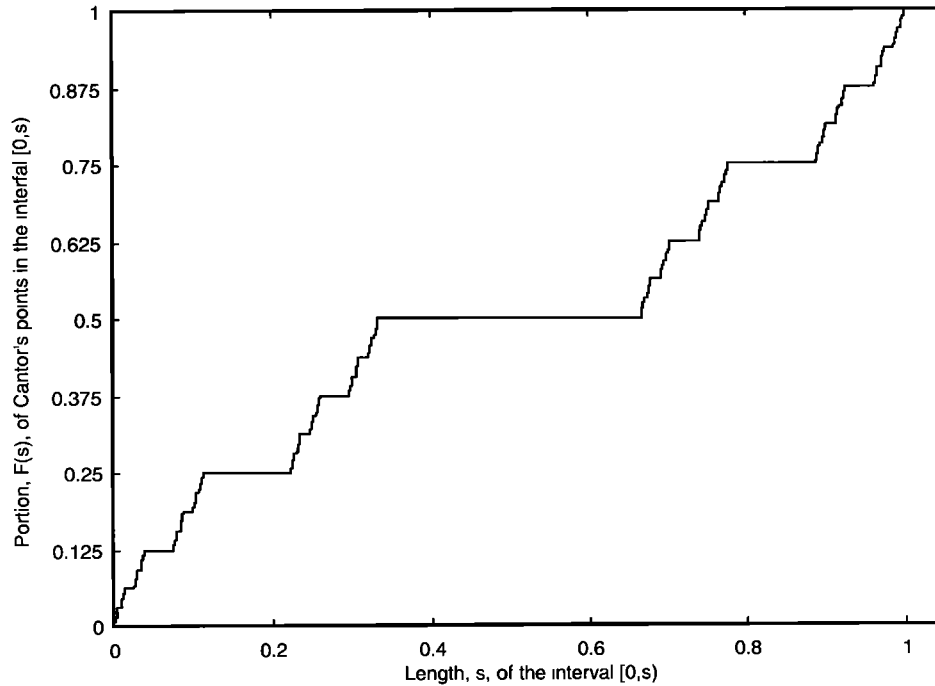
Figure 7. Distribution function of Cantor's points.

result of this theory can be used to derive the relative leaf distribution function for our fractal tree model.

Consider a function $l_\varepsilon(p)$ (in m^p) of the positive variable p defined as

$$l_\varepsilon(p) = \sum_{i=1}^{N_\varepsilon} \chi_{\varepsilon,i} \varepsilon^p , \quad p > 0 \quad (\text{in } m^p), \quad (11)$$

where N_ε and $\chi_{\varepsilon,i}$ are as in section 2.3. Let $l(p)$ be the limit of $l_\varepsilon(p)$ as the cell size ε tends to zero. This function can only take on three values: infinity if $0 < p < D$, a nonzero finite value if $p = D$, and zero if $p > D$ [*Barnsley*, 1993]. A point $p=D$ at which the jump to infinity occurs is defined to be the Hausdorf dimension. In many practically important cases (and our fractal tree models are among them), the fractal dimension (5) coincides with the Hausdorf dimension [*Barnsley*, 1993]. Therefore knowing the fractal dimension of our trees, we can approach its relative foliage area distribution function as

$$F_\varepsilon(V,D) = \frac{1}{l_\varepsilon(D)} \sum \chi_\varepsilon(r) \varepsilon^D \quad (\text{dimensionless}), \quad (12)$$

where V is a domain in the tree crown, and the summation is performed over all cells in V.

This result allows us to generalize the concept of length, surface, and volume. Indeed, the value ε^p can be interpreted as a specific volume (area, or length) of the fine cell and the value of $l(p)$ at the point $p = D$ at which the jump to infinity occurs as the generalized volume (area, or length) of a set consisting of these cells. For example, the unit Cantor set has the generalized "length" of $l(0.63) = 1 \text{ m}^{0.63}$. It follows from (4) and from Figure 5 that the value of $l(1.737) = 227.9$ (in $m^{1.737}$) can now be assigned to the crown volume of our larg-

est fractal tree. It can be shown that the fractal dimension of the tree crown space simulated by a homogeneous geometrical figure (e.g., a cylinder, or a cone) is 3. In this case, the crown volume in true sense and the generalized volume $l(3)$ (in m^3) are the same. The Hausdorf integration technique therefore in no way conflicts with the one we usually use. On the other hand, the scope of integration is extended since there exist functions integrable in the Hausdorf sense (e.g., the indicator functions of the Cantor set and of our fractal trees) for which the classical definition of integral, as demonstrated in the previous section, fails.

It is customary to write (12) and its limit (as ε tends zero) in the following generalized form:

$$F_\varepsilon(V,D) = \frac{1}{l_\varepsilon(D)} \sum \chi_\varepsilon(r) \mu(dr) ,$$

$$F(V,D) = \frac{1}{l(D)} \int_V \chi(r) \mu(dr), \quad (13)$$

where $\mu(dr)$ is the Hausdorf measure (or a specific volume) of an elementary volume (fine cell, or area, or length) about the point r. For the examples mentioned above, this measure is expressed as $\mu(dr) = (ds)^{0.63} = \varepsilon^{0.63}$ for the Cantor set; $\mu(dr) = (dxdydz)^{1.737/3} = \varepsilon^{1.737}$ for the tree crown space of the largest fractal tree class, and $\mu(dr) = dxdydz = \varepsilon^3$ for tree crowns simulated by geometrical figures. Let $V = e_i$ in (13), and as the size ε of the cell e_i about r tends to zero, we obtain a relative density distribution function $\Phi(r,D)$ of the fractal-like set at r as

$$\Phi(r,D) = \lim_{\varepsilon \to 0} \frac{F_\varepsilon(e_i,D)}{\mu(dr)} = \lim_{\varepsilon \to 0} \frac{F_\varepsilon(e_i,D)}{\varepsilon^D} = \frac{1}{l(D)} \chi(r) \text{ (in } m^{-d}\text{)};$$

that is, a portion of a fractal-like set, per elementary volume, about the space point r is proportional to the indicator function of this set.

This approach allows us to formulate the concept of generalized leaf area density distribution function as follows: Consider an elementary volume e_i about r in the tree crown. Given the total one-side leaf area S (in m^2) of the tree crown, the leaf area density distribution function $u(r,D)$ can be determined as the ratio of the one-side leaf area $S \Phi(r,D) \mu(dr)$ in the elementary volume about r to the generalized volume $\mu(dr)$ of this elementary volume; that is,

$$u(r,D) = S\,\Phi(r,D) = \frac{S}{l(D)}\chi(r) \quad \text{(in } m^2/m^d\text{)}; \quad (14)$$

that is, this function is proportional to the indicator function of the tree crown. Note that the leaf area density distribution function depends on the fractal dimension D of tree crown which is determined by within-crown leaf organization and may vary between trees [*Zeide and Pfeifer*, 1991].

Thus the Hausdorf integration technique gives us a possibility to express canopy structure both quantitatively and qualitatively. Note that we have outlined this approach without precise mathematical argumentation. It refers, for example, to (12); in the general case the fractal dimension of a fractal set bounded by the domain V may differ from one derived from (11) and hence $F(V,D)$ may not be a meaningful function. The problem of specifying a strict mathematical description of the whole approach and of incorporating it into a particular research theme is the topic of another investigation.

5. Radiative Transfer and Photosynthesis in Turbid and Fractal Media

We consider the following model of fractal canopy organization: The canopy space is a parallelepiped of height H (in meters) and basal area σ (in square meters). The canopy consists of horizontal planes with optically black, flat linear elements, horizontally oriented and uniformly distributed. The leaf area density of planes (the total one-side leaf area in the plane per unit plane area) is assumed constant. Further, there are no leaves in between these planes. Two different patterns of vertical distribution of the planes will be analyzed here.

Let the canopy be illuminated from above by a beam perpendicular to the horizontal plane $h = 0$ (Figure 8). We assume no mutual shading between leaves when viewed along the beam path. Average radiation attenuation along the beam path can be described by the following differential equation:

$$dI = -I(h)\,dS(h), \qquad I(0) = I_0 , \qquad (15)$$

where $I(h)$ is the intensity of the light beam at the depth h; $S(h)$ is the cumulative leaf area index at h (total one-side leaf area above h per unit ground area, dimensionless), and I_0 is the intensity of incident radiation. Its solution is

$$I(h) = I_0 \exp(-S(h)). \qquad (16)$$

Assuming an invariant photosynthetic response P_{leaf} of a foliage surface element as well as taking into account (15)

and (16), the rate of canopy photosynthesis, P_c can be formally expressed as [*Oker-Blom et al.*, 1991]

$$P_c = \int_0^1 P_{leaf}(I(h))dS(h) = \int_{I(H)}^{I_0} P_{leaf}(I)\frac{dI}{I} = \int_{T(H)}^1 P_{leaf}(I_0\,T)\frac{dT}{T} , \qquad (17)$$

where $T(h)$ is the canopy transmittance, $T(h) = I(h)/I_0 = \exp[-S(h)]$.

Thus the canopy transmittance and photosynthesis can be evaluated when the cumulative leaf area index is specified. We derive this variable for two different vertical distributions of the above mentioned horizontal planes. In the first case, the foliated planes are assumed to be uniformly distributed along the vertical within a layer $[0,H]$. We term this canopy organization a turbid medium. In the second case, the vertical distribution of the foliated planes in $[0,H]$ coincides with the distribution of Cantor's points iterated from the interval $[0,H]$ (Figure 8). We call this canopy a Cantor medium.

Our analysis will be performed in terms of the generalized volume discussed previously. In order to derive this variable, we introduce a fine spatial mesh as in section 2.2. Note that the total number of fine cells N_ε and the size ε of an individual cell are related by the following equation:

$$\varepsilon^3 = \frac{H\sigma}{N_\varepsilon} , \qquad (18)$$

where $H\sigma$ is the volume (in cubic meters) of our canopy space. This equation has a simple interpretation: the volume of an individual cell is the ratio of the volume of our canopy to the total number of cells constituting the canopy space.

5.1. Turbid medium.

Cells with foliage are uniformly distributed within the canopy space and therefore the indicator function takes on the
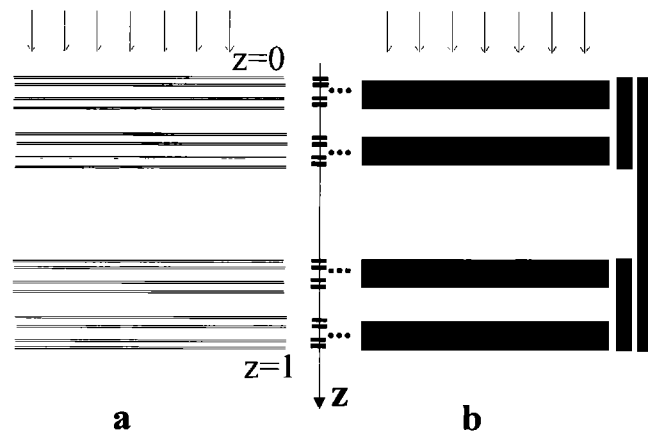

Figure 8. Horizontally homogeneous fractal model of canopy organization. The canopy space consists of horizontal planes with plane leaves, horizontally oriented, and uniformly distributed. The vertical distribution of these foliated planes coincides with distribution of Cantor's points along the OZ axis. Three successive iterations of our fractal model of canopy organization.

value 1 at any space point within the canopy space. Taking into account (18), we can rewrite (11) as

$$I_\varepsilon(p) = N_\varepsilon \, \varepsilon^p = \frac{H\sigma}{\varepsilon^3} \varepsilon^p = H\sigma \varepsilon^{p-3} \, .$$

It is clear that $I_\varepsilon(p)$ takes a finite value; that is, $H\sigma$ (in cubic meters), if and only if $p = 3$. The volume, in the true sense, therefore coincides with the volume of leaves. Let LAI_B be the leaf area index (the total one-side leaf area in the canopy space per unit ground area). It follows from (14) that the leaf area density distribution function is

$$u(r,3) = \frac{LAI_B \, \sigma}{l(3)} = \frac{LAI_B \, \sigma}{H\sigma} = \frac{LAI_B}{H} \qquad \text{(in m}^{-1}\text{)}.$$

Thus the cumulative leaf area index $S_B(h)$ for the turbid medium has the following form:

$$S_B(h) = LAI_B \, \frac{h}{H} = LAI_B \, F(s,1) \, . \qquad (19)$$

Here $F(s,1) = s$ is the relative foliage distribution function for the turbid medium; $s = h/H$ is the length of the interval $[0,h)$ in relative units. Note that the fractal dimension of the whole interval $[0,H]$, compare (5) and (18), is 1. To emphasize this, we include this value in the argument list of the distribution function.

5.2. Cantor Medium

The total number of horizontal layers of length ε containing the foliated planes coincides with number, $M_{\varepsilon,C}$, of intervals of the same length, ε, along the vertical axis containing Cantor's points (Figure 6). Consider the situation when the size ε of a cell can take on the values $H/3^n$, $n = 1, 2, \ldots$, only. In this case, we have (Figure 8) $M_{\varepsilon,C} = 2^n = (3^n)^D = (H/\varepsilon)^D$, where $D = \log_3 2$ is the fractal dimension of the Cantor set. Because leaves are uniformly distributed over the horizontal planes, each foliated layer contains σ/ε^2 cells. Thus the total number of foliated cells $N_{\varepsilon,f}$ can be expressed as $N_{\varepsilon,f} = (\sigma/\varepsilon^2)(H/\varepsilon)^D = \sigma H^D \varepsilon^{-(2+D)}$. It follows from this relationship that (11) can be rewritten as

$$I_\varepsilon(p) = N_{\varepsilon,f} \, \varepsilon^p = \sigma \, H^D \, \varepsilon^{p-2-D} \qquad \text{(in m}^p\text{)}.$$

This function can take a finite value, i.e., σH^D (in m^{2+D}), if and only if $p = 2 + D$. Therefore the generalized volume of leaves in our canopy space is

$$I_\varepsilon(2+D) = \sigma H^D \qquad \text{(in m}^{2+D}\text{)}.$$

Because the function $I_\varepsilon(2+D)$ converges to $l(2+D)$, no matter how ε tends to zero, this result does not depend on a specific choice for the size of the cell.

Let LAI_C be the leaf area index of the Cantor medium. It follows from (14) that the generalized leaf area density distribution function (in m^{-D}) has the following form:

$$u(r,2+D) = \frac{\sigma \, LAI_C}{l(2+D)} \chi(r) = \frac{\sigma \, LAI_C}{\sigma \, H^D} \chi(h) = \frac{LAI_C}{H^D} \chi(h)$$

Because leaves are uniformly distributed over horizontal

planes, the indicator function of the Cantor medium does not depend on the horizontal coordinates. Its vertical dependence coincides with the indicator function of the Cantor set iterated from the interval $[0,H]$. Taking into account (8) and (10), one can derive the cumulative leaf area index $S_C(h)$ of the Cantor medium

$$S_C(h) = \int_0^h \frac{LAI_C}{H^D} \chi(h)\mu(dh) = \int_0^h \frac{LAI_C}{H^D} dF(h)$$

$$= \frac{LAI_C}{H^D} F(h) = LAI_C \, F(s,D) \qquad (20)$$

where $\mu(dh)$ is the Hausdorf measure of an elementary interval $[h,h+dh)$; that is, $\mu(dh) = (dh)^D$ (in m^D); $F(s,D)$ is the relative distribution function of the unit Cantor set introduced in section 4 (we include the fractal dimension D in its argument list here), and $s = h/H$ is the length of the interval $[0,h)$ in relative units. It follows from (20) and (10) that the function $S_C(h)$ coincides with the distribution function of Cantor's points iterated from the interval $[0,1]$ of the length $LAI_C^{1/D}$ expressed in relative units $LAI_C^{1/D} h/H$. Therefore if the leaf area index of the turbid medium is taken as the length of the interval $[0,1]$ in relative units $L=LAI_B \, h/H$, then the leaf area index for the Cantor medium can be expressed as

$$LAI_C = (LAI_B)^D \, ,$$

where D is the fractal dimension of the Cantor set. This equation has a simple interpretation: removing the foliated planes from the turbid medium by means of the iterative procedure shown in Figure 8 involves the alteration in the leaf area index from the value of LAI_B (for the turbid medium) to $(LAI_B)^D$ (for the Cantor medium).

The canopy transmittance $T(h,D)$ of the media takes the form

$$T(h,D) = \exp(-S(h)) = \exp(-LAI_B^D \, F(s,D)), \qquad (21)$$

where $F(s,D)$ is the relative plane distribution function for the layer $[0,H]$. Inserting this in (17), we obtain an expression for canopy photosynthesis

$$P(D) = \int_{\exp(-LAI_B^D)}^1 P_{\text{leaf}}(I_0 \, T)\frac{dT}{T} \, . \qquad (22)$$

Thus if the turbid medium is replaced by the Cantor medium, canopy transmittance and photosynthesis will change from $T(h,1)$ and $P(1)$ to $T(h,\log_2 3)$ and $P(\log_3 2)$.

It follows from (21) that the relationship between leaf area index and transmittance of a canopy can be expressed in the form of Beer's law, irrespective of the internal organization of the canopy; that is,

$$T(H,D) = \exp(-LAI), \qquad (23)$$

where $LAI = LAI_B$ for the turbid medium and $LAI = LAI_C$ for the Cantor medium. Therefore in the case of horizontally homogeneous media, it follows that canopy transmittance can be predicted by Beer's law irrespective of the canopy organiza-

tion. This, however, leads to erroneous estimation of leaf area index when the Beer's law is inverted. Indeed, one can measure canopy transmittance without making any assumption about canopy organization. The leaf area index thus derived from (23) does not depend on such assumptions too. In using this technique therefore, the important thing is to recognize the canopy organization to which the derived LAI refers. Let us suppose that the leaf area index derived corresponds to the Cantor medium. In this case, its nth approximation contains 2^n foliated layers of the height $\varepsilon = H/3^n$ each (compared to turbid medium which contains 3^n foliated layers of the height $\varepsilon = H/3^n$ each). Let us remove all nonfoliated layers and change each foliated layer by powering its height by $D = \log_3 2$. As a result of this transformation, the new medium has 2^n foliated layers of the height $\varepsilon = H^D/2^n$ each. These layers are now uniformly distributed along the vertical within the layer $[0, H^D]$. Thus the Cantor medium of depth H and leaf area index LAI_C corresponds to the turbid medium of depth H^D and the same leaf area index LAI_C. Therefore if we want to treat this Cantor medium of depth H as a turbid medium of the same depth, then we should assign the value $LAI^{1/D}$ to its leaf area index. Note that the same result was derived by analyzing (19) and (20). Such a correction of measured LAI is required before its use as input for any canopy radiation model based on Beer's law.

Neglecting internal canopy organization also leads to errors in estimated canopy photosynthesis. The Cantor canopy is equivalent to the turbid medium of $LAI_C^{1/D}$. Thus the Cantor medium which contains leaves of area σLAI_C takes up as much CO_2 as the turbid medium with leaves of area $\sigma LAI_C^{1/D}$. This follows from (22) also.

6. Summary

The architecture of a vegetation canopy is the most important factor determining the canopy radiation regime. All canopy radiation models therefore require the probability distribution function of leaf area in order to specify statistical features of canopy architecture. In probability theory [*Kolmogorov*, 1950], any distribution function F can be represented as a sum of three components: $F = \alpha C + \beta J + \gamma S$ where α, β, and γ take on the values 0 or 1 depending on whether or not the corresponding component is represented. The first summand C is the continuous probability distribution function. The uniform, Gaussian, gamma, etc., distributions are examples of this component. The second summand J is the jump function. This is a piece-wise constant function which describes random discrete variables taking on finite or countably infinite number of values. The third summand S is the singular function. It is a continuous, nonconstant function whose derivative is zero almost everywhere.

Previous canopy radiation models used the first and second components to describe the structure of vegetation canopies which allows us to mathematically express radiation attenuation by Beer's law. This predetermines the scale at which it provides an adequate prediction. This is the landscape scale, which can account for spatial distribution of trees, tree shape, the mean vertical or/and horizontal distribu-

tions of foliage within crowns, clumping, and mean leaf size, but which ignores small-scale structural features of canopy organization. In the present paper, we considered examples of fractal-like canopy organizations, in which the spatial distribution of phytoelements is described by singular probability distribution functions. Any attempt to use continuous and discrete distribution functions leads to degeneration in the description of canopy structure. The use of the singular distribution function therefore is needed in order to derive the distribution of phytoelements. However, one requires information about fractal characteristics of the vegetation canopy to do this. The singular distribution function assumes that the foliage elements in an elementary volume are uniformly distributed and generally obtained by powering a unit elementary volume by a fractal dimension. Because photosynthesis in an elementary volume depends on the distribution of radiation on foliage elements, this property of fractal-like canopy organization influences photosynthesis of the entire vegetation canopy. The fractal dimension depends on the structure of tree organization and may vary between trees and tree species. Thus canopy radiation models based on continuous and discrete distribution functions are unable to account for such features of canopy organization. The use of the singular distribution function in canopy radiation models, however, requires information on fractal characteristics of trees and tree communities. Their measurement and modeling therefore requires special attention in order to extend the applicability of Beer's law.

References

Barnsley, M. F., *Fractals Everywhere*, 531 pp., Academic, San Diego, Calif., 1993.

Carlson, B. G., Transport theory: Discrete ordinates quadrature over the unit sphere, *LANL Rep. LA-4554*, Los Alamos Nat. Lab., N.M., 1970.

Chen, S. G., B.Y. Shao, I. Impens, and R. Ceulemans, Effect of plant canopy structure on light interception and photosynthesis, *J. Quant. Spectrosc Radiat. Transfer*, 52, 115-123, 1994.

de Reffye, P., P. Dinouard, and D. Barthélémy, Modélisation et simulation de l'architecture de l'orme du japon Zelkova Serrata (Thunb.) Makino (Ulmaceae): La notion d'axe de référence, in *Naturalia Monspeliensia*, pp. 251-266, CIRAD, Montpellier, France, 1991.

Ehlinger, J.R., and C.B. Field (Eds.), *Scaling physiological processes: Leaf to globe*, Academic, San Diego, Calif., 1993.

Gruber, F., J. Heimann, and A. Thorwest, Jahresbericht zum BMFT Teilprojekt PI-1.2: Die hydraulische Architektur der Fichte, *Ber. Forschungszent. Waldökosyst.*, Ser. B., vol. 31, pp. 259-279, 1992.

Knyazikhin, Y., G. Miessen, O. Panfyorov, and G. Gravenhorst, Small-scale study of three-dimensional distribution of photosynthetically active radiation in a forest, *Agric. For. Meteorol.*, in press, 1997.

Kolmogorov, A. M., *Foundations of the Theory of Probability*, 71 pp., Chelsea, New York, 1950.

Kranigk, J., *Ein Model für den Strahlungstransport in Fichtenbeständen*, 127 pp., Cuvillier, Göttingen, Germany, 1996.

Kranigk, J., and G. Gravenhorst, Ein dreidimensionales Modell für Fichtenkronen, *Allg. Forst Jagdztg.*, 164 (8), 146-149, 1993.

Kranigk, J., F. Gruber, J. Heimann, and A. Thorwest, Ein Model für die Kronenraumstruktur und die räumliche Verteilung der

Nadeloberfläche in einem Fichtenbestand, *Allg. Forst Jagdztg., 165* (10-11), 193-197, 1994.

Li, X., and A. H. Strahler, Geometrical-optical bidirectional reflectance modeling of a conifer forest canopy, *IEEE Trans. Geosci. Remote Sens., 24*, 906-919, 1986.

Li, X., A. Strahler, and C. E. Woodcock, A hybrid geometric optical-radiative transfer approach for modelling albedo and directional reflectance of discontinuous canopies, *IEEE Trans. Geosci. Remote Sens., 2*, 466-480, 1995.

Lovejoy, S., and D. Schetzer, How bright is the coast of Brittany?, in *Fractals in Geoscience and Remote Sensing*, pp. 102-151, edited by G.G. Wilkinson, I. Kanellopoulos, and J. Mègier, Off. for Off. Publ. of the Eur. Communities, Luxembourg, Belgium, 1994.

Monsi, M., and T. Saeki, Über den Lichtfaktor in den Pflanzengesellschaften und seine Bedeutung für die Stoffproduktion, *Jpn., J. Bot., 14*, 22-52, 1953.

Myneni, R. B., G. Asrar, and S. A. W. Gerstl, Radiative transfer in three dimensional leaf canopies, *Transp. Theor. Stat. Phys., 19*, 205-250, 1990.

Nilson, T., A theory of radiation penetration into non-homogeneous plant canopies, in *The Penetration of Solar Radiation Into Plant Canopies*, pp. 5-70, *Estonian* Acad. Sci., Tartu, Estonia, 1977.

Nilson, T., Radiative transfer in nonhomogeneous plant canopies, in *Advances in Bioclimatology*, edited by G. Stanhill, vol. 1, pp. 59-88, Springer-Verlag, New York, 1992.

Norman, J.M., and J. M. Welles, Radiative transfer in an array of canopies, *Agron. J., 75*, 481-488, 1983.

Oker-Blom, P., J. Lappi., and H. Smolander, Radiation regime and photosynthesis of coniferous stands, in *Photon-Vegetation Interactions: Applications in Plant Physiology and Optical Remote Sensing*, pp. 469-499, edited by R. B. Myneni and J. Ross, Springer-Verlag, New York, 1991.

Prioul, J.L., and P. Chartier, Partitioning of transfer and carboxylation components of intracellular resistance to photosynthetic CO_2 fixation: A critical analysis of the methods used, *Ann. Bot., 41*, 789-800, 1977.

Quattrochi, D.A., and M.F. Goodchild (Eds.), *Scale in Remote Sensing and GIS*, CRC/Lewis, Boca Raton, Fla., 1997.

Rigon, R., A. Rinaldo, and I. Rodrigueziturbe, On landscape self-organization, *J. Geophys. Res.*, 99, 11,971-11,993, 1994.

Ross, J., *The Radiation Regime and Architecture of Plant Stands*, 391 pp., Dr. W. Junk, Norwell, Mass., 1981.

Ross, J., and T. Nilson, The calculation of photosynthetically active radiation in plant comminities, in *Solar Radiation Regime in Plant Stands*, pp. 5-54, *Estonian* Acad. Sci., Inst. Phys. Astron, Tartu, Estonia, 1968.

Stenberg, P., Penumbra in within-shoot and between-shoot shading in conifers and its significance for photosynthesis, *Ecol. Modell.*, 77, 215-231, 1995.

Vedyushkin, M., Fractal characteristics of forest spatial structure, *Vegetatio, 113*(1), 65-70, 1995.

Zeide, B., and P. Pfeifer, P., A method for estimation of fractal dimension of tree crown, *For. Sci., 37*, 1253-1265, 1991.

G. Gravenhorst, J. Kranigk, and O. Panfyorov, Institute of Bioclimatology, University Göttingen, Büsgenweg 2, D-37077, Göttingen, Germany. (e-mail: ggraven@gwdg.de; opanfyo@gwdg.de)

Y. Knyazikhin, R. B. Myneni, Dep. of Geography, Boston University, 675 Commonwealth Avenue, Boston, MA 02215 (e-mail: jknjazi@crsa.bu.edu; rmyneni@crsa.bu.edu)